Detlef MAIER[1]
Zheng SUN[2]

ON BOARD CONDITION MONITORING OF FEED AXES BY SIGNAL DECOMPOSITION FOR MACHINES WITH BALL SCREW DRIVES

In order to establish a condition monitoring system to detect wear of the mechanical components of feed drives with ball screws a measuring and data evaluation method has been established. In order to keep the costs down, boundary condition is to use the machines own functionalities only (On Board Diagnosis). At present, most of wear detecting methods use vibration analysis. Here, a signal analysis method is presented that may well complement established methods of vibration analysis. The publication presents a method to exploit positioning data to detect wear of a ball screw drive exemplarily that is run under real conditions. The presented method is partially derived from wear detection methods of roller bearings and may also be adapted for other parts such as linear guides.

1. INTRODUCTION AND MOTIVATION

Machine tools contain a multitude of components, some of which are critical for the operation. In particular this is true for feed axes. Therefore there is a big application potential for diagnostics. So far, only for expensive machine tools there were cost effective applications. But, from the operators point of view it is desirable to expand the diagnostic on other components the diagnostic of which was not yet cost effective. For every component the failure probability is fed into some kind of risk analysis. From the user's point of view it's best if the diagnostics and the risk analysis is part of the supplied functionality of the machine tool. Long since the pervasive spread of information technology has reached machine tools. The data processing units complement the mechanical units to form an integrated functional system. The whole functionality of the system will define the market value of the machine. In the long term high surcharges for additional electronic functions may not be accomplished. Therefore a diagnostic system should imbed in the machine itself.

---

[1] Academic staff of the Institut fuer Werkzeugmaschinen (IfW), Universaet Stuttgart, Germany
(Corresponding Author), (Sponsor: Prof. U. Heisel)
[2] Graduand at the same Institute, ministered by Dipl.-Ing. Detlef Maier

When the machines sensors only may be used, the states of all mechanical components together influence the available signals of the machines controller at the same time. To identify the worn or damaged component such as bearings, linear guides or ball screws the component's particular contribution to the summoned signal has to be identified and separated. Therefore the available signals have to be decomposed.

Here, the positioning signal will be investigated. After that the separated portions of the signals have to be assigned to the according components. Preliminarily the sampled signals must bear the according information. Thus in the forehand the signals have to be captured under specific conditions. If a cost effective detection of wear of the feed drive's components has to be achieved, it is desirable not to interrupt the production. During signal acquisition, it is not always possible. When the preconditions for the signal acquisition are not met accordingly, the quality of the signal may not suffice. Hereafter an approach is presented, how the preconditions for data acquisition and how to decompose signals may be derived from a component's kinematics. Exemplarily a ball screw is examined. It was chosen, because from the above mentioned components it has the most complex kinematics. Also, for bearings the according methods are already well known. For linear guides, the presented approach may be adopted. As a proof of concept, an experiment was conducted. It shows that the according information may be separated from the positioning signal. To complement the approach, a possibility is shown how the development of wear may be derived from acquired signals.

2. SIGNAL DECOMPOSITION BY INVESTIGATION OF THE KINEMATICS OF BALL SCREW DRIVES

First, if a signal-decomposition and an extraction and an interpretation of the portions have to be conducted, it's important to know what to look for i.e. to find out which portion of the signal bears the concerning information. The results of Palmgren's investigations of roller bearings [1] are well known as *"characteristic frequencies"*. Meanwhile they are common figures that are available in the specifications of bearing catalogues. Not only for a machine based analysis, for sensor-based analyses too, the characteristic frequencies of a ball screw have to be separated from a signal that summons the concerted operation of all mechanical components of the whole feed drive. Even if the sensor is placed in the very close vicinity of the respective part that does not at all mean that the recorded signal is not a summoned signal. In the real world, a kinematic system may not really be cut free from its environment.

Hereafter a ball screw was chosen as an example. Inside it a kinematic interaction of the rolling contact components happens. The relative velocity of all parts may be calculated. The derivation of the calculation is already due to be published by its author elsewhere [] in the very moment this article is being written. Since it was not published yet, with kind permission of its author, here it is quoted in a translated and shortened version. Then, afterwards a second approach is presented.

For calculating the characteristic frequencies of a ball screw as a first approximation a few prerequisites are supposed:

- The balls do roll ideally
- No sliding friction occurs
- The balls do not bore
- The calculations are done for two-dimensional coordinates only
- Some geometric relations are approximated
- All equations are solved algebraically

2.1. CHARACTERISTIC FREQUENCIES OF A BALL SCREW
(FIRST APPROXIMATION)
[*Begin of citation of Michael Walther [2]*]

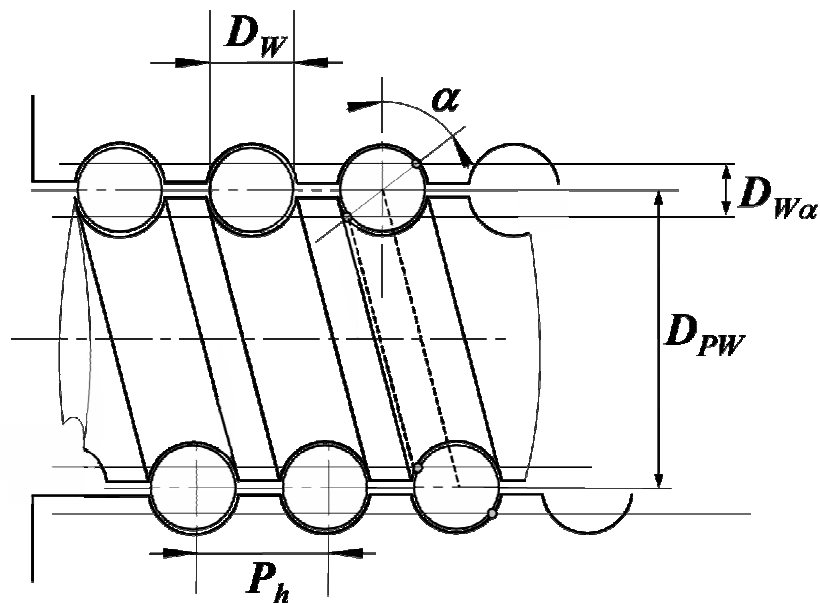Fig. 1 shows the relevant measurements of a ball screw.

Fig. 1. Measurements of a ball screw

The balls' centres move on a helix. Its length l_{pw} and the actual rolling circle of the balls $D_{w\alpha}$ are:

$$l_{pw} = \sqrt{(\pi \cdot D_{pw})^2 + P_h{}^2} \qquad D_{w\alpha} = D_w \cdot \cos\alpha \qquad (1), (2)$$

The lenghts of the contacts runways in the nut and on the shaft are:

$$l_{pw,Mutter} = \sqrt{((D_{pw} + D_w \cdot \cos \alpha) \cdot \pi)^2 + P_h{}^2} \quad l_{pw,Spindel} = \sqrt{((D_{pw} - D_w \cdot \cos \alpha) \cdot \pi)^2 + P_h{}^2} \quad (3), (4)$$

Fig. 2. shows the kinematic and geometric relations inside the ball screw nut. Physically, the rolling action is described as a movement around the velocity pole.
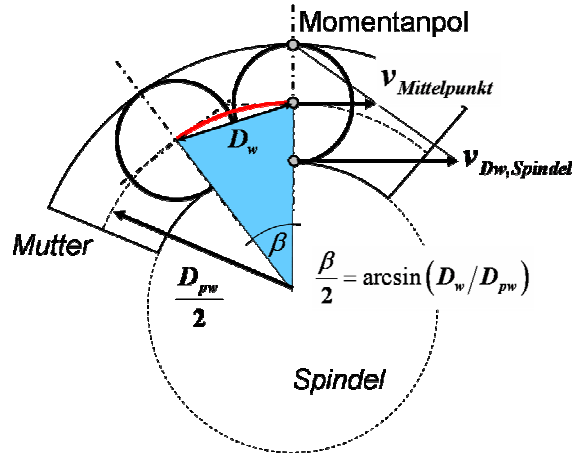

Fig. 2. Model for the kinematic calculation of the ball's velocities and the packaging of the balls

To calculate the velocity of the ball's centre the theorem on intersecting lines is used:

$$v_{Mittelpunkt} \big/ v_{Dw,Spindel} = 1\big/2 \tag{5}$$

The velocity $v_{DW,Spindel}$ of the contact point at the shaft is:

$$v_{Dw,Spindel} = f_{Spindel} \cdot l_{pw,Spindel} = f_{Spindel} \cdot \sqrt{((D_{pw} - D_w \cdot \cos \alpha) \cdot \pi)^2 + P_h{}^2} \tag{6}$$

The duration t_{Umlauf} of one total circulation of the ball around the shaft is:

$$t_{Umlauf} = \frac{l_{pw}}{v_{Mittelpunkt}} = \frac{2 \cdot \sqrt{(\pi \cdot D_{pw})^2 + P_h{}^2}}{f_{Spindel} \cdot (D_{pw} - D_w \cdot \cos \alpha)} \tag{7}$$

It's common to refer the result to the rotational frequency $f_{Spindel}$ of the shaft:

$$f_{Umlauf} = \frac{1}{t_{Umlauf}} = f_{Spindel} \cdot \frac{\sqrt{((D_{pw} - D_w \cdot \cos \alpha) \cdot \pi)^2 + P_h{}^2}}{2 \cdot \sqrt{(\pi \cdot D_{pw})^2 + P_h{}^2}} \tag{8}$$

In a plane packaging the centres of two balls cover the segment β of a circle. Therefore, the number of balls z is:

$$z = 2\pi/\beta \quad \beta = 2 \cdot \arcsin\left(D_w/D_{pw}\right) \qquad (9); (10)$$

If the helix is projected in the plane z balls fit in the circle:

$$z = \frac{\pi}{\arcsin\left(D_w/D_{pw}\right)} \qquad (11)$$

The balls are arranged on a helix. Its actual length may be calculated if the lead (pitch) P_h is taken into account. It's important, that z must *not* in every case be a natural number of course:

$$z = \frac{l_{pw}}{D_{pw} \cdot \beta} = \frac{\sqrt{(\pi \cdot D_{pw})^2 + P_h{}^2}}{D_{pw} \cdot 2 \cdot \arcsin\left(D_w/D_{pw}\right)} \qquad (12)$$

A location in the nut, for example the re-feeding unit is passed z times per turn. Therefore, the re-feeding frequency $f_{Austritt}$ is:

$$f_{Austritt} = f_{Umlauf} \cdot z = f_{Spindel} \cdot \frac{\sqrt{((D_{pw} - D_w \cdot \cos\alpha) \cdot \pi)^2 + P_h{}^2}}{2 \cdot \sqrt{(\pi \cdot D_{pw})^2 + P_h{}^2}} \cdot \frac{\sqrt{(\pi \cdot D_{pw})^2 + P_h{}^2}}{D_{pw} \cdot 2 \cdot \arcsin\left(D_w/D_{pw}\right)} \qquad (13)$$

$$f_{Austritt} = f_{Spindel} \cdot \frac{\sqrt{((D_{pw} - D_w \cdot \cos\alpha) \cdot \pi)^2 + P_h{}^2}}{D_{pw} \cdot 2 \cdot \arcsin\left(D_w/D_{pw}\right)}$$

A location on the shaft is passed with the inner frequency f_{innen}:

$$f_{innen} = f_{Spindel} \cdot \frac{\sqrt{((D_{pw} + D_w \cdot \cos\alpha) \cdot \pi)^2 + P_h{}^2}}{2 \cdot \sqrt{(\pi \cdot D_{pw})^2 + P_h{}^2}} \cdot \frac{\sqrt{(\pi \cdot D_{pw})^2 + P_h{}^2}}{D_{pw} \cdot 2 \cdot \arcsin\left(D_w/D_{pw}\right)} \qquad (14)$$

$$f_{innen} = f_{Spindel} \cdot \frac{\sqrt{((D_{pw} + D_w \cdot \cos\alpha) \cdot \pi)^2 + P_h{}^2}}{D_{pw} \cdot 2 \cdot \arcsin\left(D_w/D_{pw}\right)}$$

[*End of citation of Michael Walther [2]*]

2.2. CHARACTERISTIC FIGURES OF A BALL SCREW
(SECOND APPROXIMATION)

To conduct the second approximation some prerequisites have changed:
- The balls do not roll ideally
- Sliding friction occurs
- The balls do bore
- The calculations are done for three-dimensional coordinates
- Some geometric relations are (still) approximated
- Equations are solved numerically also

The leading (pitch) angle ψ_{pw} is:

$$\psi_{pw} = \arctan\left(\frac{P_h}{\pi \cdot D_{pw}}\right) \tag{15}$$

The trajectory of the runway of the ball's contact point at the nut has the length $l_{pw.\,Nut}$:

$$l_{pw,\,Nut} = \sqrt{\left(D_{pw} + D_w \cdot \cos\alpha\right)^2 + \left(D_w \cdot \sin\alpha \cdot \sin\psi_{pw}\right)^2} \tag{16}$$

For the shaft the length $l_{pw.\,Sp}$ is:

$$l_{pw,\,Sp} = \sqrt{\left(D_{pw} - D_w \cdot \cos\alpha\right)^2 + \left(D_w \cdot \sin\alpha \cdot \sin\psi_{pw}\right)^2} \tag{17}$$

The velocity pole is considered to coincide with the contact point A at the nut (Fig. 3).
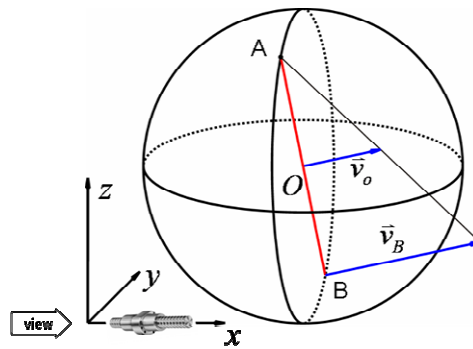

Fig. 3. Velocities of the ball's contact points and its centre

The theorem on intersecting lines applied on Fig. 3 delivers the ratio of the norm of the velocities:

$$\frac{|\vec{v}_0|}{|\vec{v}_B|} = \frac{1}{2} \tag{18}$$

The velocities of the ball's centre $\vec{v}_O$ and at the contact point $\vec{v}_{Sp}$ are:

$$\vec{v}_O = k \cdot \begin{pmatrix} D_{pw} \cdot \pi \\ P_h \\ 0 \end{pmatrix} \qquad \vec{v}_B = 2k \cdot \begin{pmatrix} D_{pw} \cdot \pi \\ P_h \\ 0 \end{pmatrix} \tag{19), (20}$$

where k is a factor that represents the geometry and the friction.
On the other hand the velocity of the rotating shaft at the contact point is (see

Fig. 5):

$$\vec{v}_{Sp} = f_{Sp} \cdot \begin{pmatrix} D_{Sp} \cdot \pi \\ P_h \\ 0 \end{pmatrix} \tag{21}$$

where f_{Sp} is the rotary frequency of the shaft.

Each of the concerning contact points has got a different angle α since the diameter and therefore the lengths of the respective helical runways are different. Especially $\vec{v}_B$ and $\vec{v}_{Sp}$ do not coincide. That means the ball does not roll ideally. An additional component $\vec{v}_{B,r}$ has to be introduced:

$$\vec{v}_{B,r} = \vec{v}_{B,a} - \vec{v}_{Sp} \tag{22}$$

It is clear, that the sliding velocity $\vec{v}_{B,r}$ depends on the friction.

Like at a car's front axle that drives through a plane curve, the inner rolling circle of the ball should be inclined further than the outer, since the inner runway's circle is narrower than the outer (Fig. 4, left). Normally, a ball screw's geometry is set up to give a symmetric contact angle (Fig. 4, centre). That means, the intersecting lines of the contact points meet in the ball's centre. Therefore, the ball's two rolling circles are forced to act like a beam axle without a differential i.e. they are tightened together, have the same rotational speed and are parallel. The inner runway is shorter than the outer. Therefore the ball makes a compensating yaw-movement ω_x. It may well be assumed, that the yawing is alternating. Thus, here the averaged influence of ω_x on the ball's velocities may be neglected.

Insert: Fig. 4, centre shows the common static setup of ball screw design. For rolling kinematics it's not optimized. As an improvement, the inner profile's halves of the nut and of the shaft respectively could be narrower and the profile could be inclined (Fig. 4, right). Thus, the ball's inner rolling circle becomes smaller. That compensates the different velocities. Ideally, the set-point of the 3D-arrangement should be the shaft's centre. As Fig.

4, right illustrates it's difficult to realize. It may be, if the balls are considerably smaller than the shaft's diameter. (The load forces wouldn't intersect in the ball's centre any more. The ball would be stressed differently. The advantages may be reduced friction).
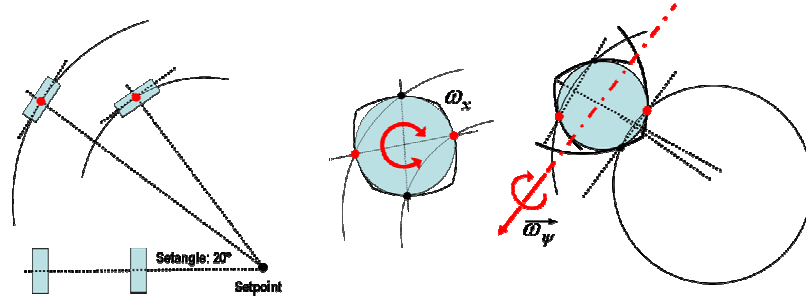

Fig. 4. Rolling kinematics of plane curves. Inclined (l.), yawing (m.) and tilting (r.) rolling angles.

On the other hand, the ball rolls due to different pitch angles ω_{ψ}. The shaft's diameter is smaller than the nut's. The pitch P_h is the same. Therefore, at the inside the ball encounters a steeper lead (pitch) angle Ψ_{Sp} than on the outside Ψ_{Nut} (like at a spiral staircase). Also the ball's centre has its own angle Ψ_{pw}:

$$\psi_{Nut} < \psi_{pw} < \psi_{Sp} \tag{23}$$

Therefore the ball is tilted also while it rolls. That results ω_{ψ}. The tilting is approximately orthogonal to its actual rolling. It's not alternating and its direction is always from inside to outside. The above considerations lead to the conclusion that a ball may never roll ideally inside a real ball screw nut. It always wobbles. The three-dimensional problem of a real ball screw is even more complex. The ball is prone to rolling, sliding *and* boring friction at different planes and axes at the same moment.
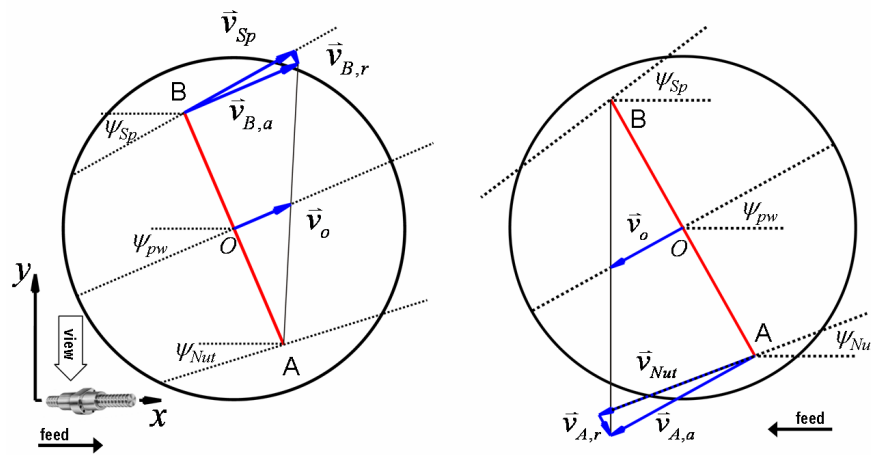

Fig. 5. Interrelation of the velocities at the ball. Assumed positions of the pole do coincide with point A (left) or with point B (right)

Now the view is at the side of the shaft, not in the middle (Fig. 5). The view coincides with the ball's tilting axis ω_ψ. To analyze the problem two cases are compared. It's assumed, the ball is instable. First, it's considered the ball rolls ideally at the nut i.e. the velocity pole coincides with the respective contact point. Second, it's considered it coincides with the shaft.

ω_ψ causes a portion of (sliding) velocity $\vec{v}_{B,r}$. The norm of $\vec{v}_{B,r}$ is:

$$\left|\vec{v}_{B,r}\right| = \left|\vec{v}_{Sp}\right| \cdot \sin\left(\psi_{Sp} - \psi_{pw}\right) = f_{Sp} \cdot \sqrt{\left(D_{Sp} \cdot \pi\right)^2 + P_h^2} \cdot \sin\left(\psi_{Sp} - \psi_{pw}\right) \tag{24}$$

The velocity of the ball's centre is:

$$\left|\vec{v}_{B,a}\right| = \frac{1}{2} \cdot f_{Sp} \cdot \sqrt{\left(D_{Sp} \cdot \pi\right)^2 + P_h^2} \cdot \cos\left(\psi_{Sp} - \psi_{pw}\right) \tag{25}$$

In the second case (see Fig. 5. right) as before, the centre of the ball runs along its helical path. Now the velocity of the contact point is:

$$\vec{v}_{Nut} = f_{Nut} \cdot \begin{pmatrix} D_{Nut} \cdot \pi \\ P_h \\ 0 \end{pmatrix} \tag{26}$$

where f_{Nut} is the rotating frequency of the nut. If the feed speed of the drive is the same as before the rotational speeds are the same $f_{Nut} = f_{Sp}$. Therefore the norm of the sliding portion of the velocity $\vec{v}_{A,r}$ is:

$$\left|\vec{v}_{A,r}\right| = f_{Sp} \cdot \sqrt{\left(D_{Nut} \cdot \pi\right)^2 + P_h^2} \cdot \sin\left(\psi_{pw} - \psi_{Nut}\right) \tag{27}$$

Now, the velocity of the ball's centre is:

$$\left|\vec{v}_{A,o}\right| = f_{Sp} \cdot \left(\sqrt{\left(D_{pw} \cdot \pi\right)^2 + P_h^2} - \frac{1}{2} \cdot \sqrt{\left(D_{Nut} \cdot \pi\right)^2 + P_h^2} \cdot \cos\left(\psi_{pw} - \psi_{Nut}\right)\right) \tag{28}$$

In fact, the velocity pole is neither in point A nor in point B. The system is instable. Thus the actual speed of the ball's centre may only be limited to a specific range:

$$\left|\vec{v}_{A,0}\right| \leq \left|\vec{v}_0\right| \leq \left|\vec{v}_{B,0}\right| \tag{29}$$

To get closer to the actual speed of the balls, the frictional forces at the respective contact points are taken into account. Now it's assumed that $\vec{v}_{A,r}$ and $\vec{v}_{B,r}$ are proportional to

friction and to each other. Since the ball moves it may also be assumed, that the proportion is not constant above time:

$$\frac{F_{fr,A}}{F_{fr,B}} = \frac{\mu_A}{\mu_B} = \frac{\left|\vec{v}_{B,r}\right|}{\left|\vec{v}_{A,r}\right|} \tag{30}$$

That means the velocities are balanced dynamically. The ball's state is a dynamic equilibrium. In simple words: low friction means a high sliding velocity. High friction means low sliding velocities. The momentary state i.e. the actual momentary velocity may not be captured. Therefore the ranges of the velocities are specified:

$$0 \le \left|\vec{v}_{A,r}\right| \le f_{Sp} \cdot \sqrt{\left(D_{Nut} \cdot \pi\right)^2 + P_h^2} \cdot \sin\left(\psi_{pw} - \psi_{Nut}\right)\left\{= \left|\vec{v}_{A,r}\right|_{\max}\right\}$$

and   (31)

$$0 \le \left|\vec{v}_{B,r}\right| \le f_{Sp} \cdot \sqrt{\left(D_{Nut} \cdot \pi\right)^2 + P_h^2} \cdot \sin\left(\psi_{Sp} - \psi_{pw}\right)\left\{= \left|\vec{v}_{B,r}\right|_{\max}\right\}$$

If there are no frictional forces at the respective point the velocity is zero. But, the velocities are bound to the kinematics. Therefore they may not exceed their range. Further it's assumed that the energy inside the moving system is dynamically balanced and the velocities are proportional to the frictional forces it may be formulated:

$$\frac{\left|\vec{v}_{A,r}\right|}{\left|\vec{v}_{A,r}\right|_{\max}} = \frac{\left|\vec{v}_{B,r}\right|_{\max} - \left|\vec{v}_{B,r}\right|}{\left|\vec{v}_{B,r}\right|_{\max}} = \frac{\left|\vec{v}_{B,r}\right|_{\max}}{\left|\vec{v}_{B,r}\right|} = k \tag{32}$$

That means if the frictional force at point A is higher the respective sliding velocity is lower and the energy is transformed to point B when the velocity of which rises (and vice versa). In other words: The closer the sliding velocity of contact point A gets to its maximum the smaller gets the remaining sliding velocity at its opposed contact point B (and vice versa). In order to determine the frictional forces, the normal forces have to be determined before. When the drive moves an axial force is imposed on the ball screw. The normal force on a ball is a portion of it:

$$F_N = \frac{F_{axial}}{\cos \alpha} \tag{33}$$

Thus the frictional force at Point A is:

$$F_{fr,A} = \frac{\mu_{Nut} \cdot F_{axial}}{\cos \alpha_{Nut}} = \mu_{Nut} \cdot F_{axial} \cdot \frac{\sqrt{\left(D_{Nut} \cdot \pi\right)^2 + P_h^2}}{D_{Nut} \cdot \pi} \tag{34}$$

At point B the frictional force is determined accordingly:

$$F_{fr,B} = \frac{\mu_{Sp} \cdot F_{axial}}{\cos \alpha_{Sp}} = \mu_{Sp} \cdot F_{axial} \cdot \frac{\sqrt{\left(D_{Sp} \cdot \pi\right)^2 + P_h^2}}{D_{Sp} \cdot \pi} \tag{35}$$

To handle the equation, k was introduced. If (34) and (35) are applied on (32) k results:

$$k = \frac{\dfrac{\left(D_{Sp} \cdot \pi\right)^2 + P_h^2}{D_{Sp} \cdot \pi} \cdot \mu_{Sp} \cdot \sin\cdot\left(\psi_{Sp} - \psi_{pw}\right)}{\dfrac{\left(D_{Sp} \cdot \pi\right)^2 + P_h^2}{D_{Sp} \cdot \pi} \cdot \mu_{Sp} \cdot \sin\cdot\left(\psi_{Sp} - \psi_{pw}\right) + \dfrac{\left(D_{Nut} \cdot \pi\right)^2 + P_h^2}{D_{Nut} \cdot \pi} \cdot \mu_{Nut} \cdot \sin\cdot\left(\psi_{pw} - \psi_{Nut}\right)} \tag{36}$$

The ball strives for the middle between the two cases. That means it reaches out for equally balanced angles $\psi_{Sp} - \psi_{pw} \approx \psi_{pw} - \psi_{Nut}$. Thus (36) may be simplified:

$$k = \frac{\dfrac{\left(D_{Sp} \cdot \pi\right)^2 + P_h^2}{D_{Sp} \cdot \pi} \cdot \mu_{Sp}}{\dfrac{\left(D_{Sp} \cdot \pi\right)^2 + P_h^2}{D_{Sp} \cdot \pi} \cdot \mu_{Sp} + \dfrac{\left(D_{Nut} \cdot \pi\right)^2 + P_h^2}{D_{Nut} \cdot \pi} \cdot \mu_{Nut}} \tag{37}$$

The velocity of the ball's centre is:

$$\left|\vec{v}_o\right| = \frac{1}{2} \cdot \left|\vec{v}_{A,a}\right| \cdot k + \frac{1}{2} \cdot \left|\vec{v}_{B,a}\right| \cdot \left(1 - k\right) \tag{38}$$

To determine the characteristic frequencies of a ball screw, it's essential to know how many balls are on the runway i.e. how close they follow each other. First it has to be examined how long the runway is. Mathematically a helix is described like this:

$$\begin{pmatrix} x \\ y \\ z \end{pmatrix} = \begin{pmatrix} \dfrac{D_{pw}}{2} \cdot \cos \gamma \\ \dfrac{D_{pw}}{2} \cdot \sin \gamma \\ \dfrac{P_h}{2\pi} \cdot \gamma \end{pmatrix} \tag{39}$$

Fig. 6 shows the unwinding of the ball's runway and its projection onto the x-y-plane.
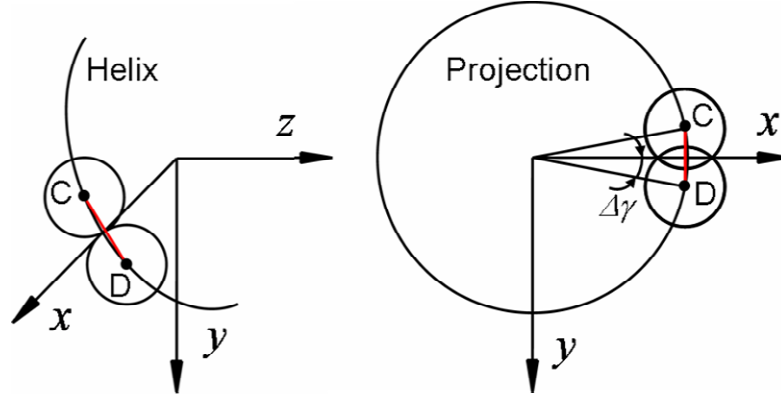
Fig. 6. Unwinding of the helical trajectory (left) and its projection on the x-y-plane (right)

In Fig. 6 $\Delta\gamma$ is half of the segment covered by the distance of two ball's centres. The coordinates of the first ball's centre are:

$$\begin{pmatrix} x_C \\ y_C \\ z_C \end{pmatrix} = \begin{pmatrix} \dfrac{D_{pw}}{2} \cdot \cos(-\Delta\gamma) \\ \dfrac{D_{pw}}{2} \cdot \sin(-\Delta\gamma) \\ \dfrac{P_h}{2\pi} \cdot (-\Delta\gamma) \end{pmatrix} = \begin{pmatrix} \dfrac{D_{pw}}{2} \cdot \cos\Delta\gamma \\ -\dfrac{D_{pw}}{2} \cdot \sin\Delta\gamma \\ -\dfrac{P_h}{2\pi} \cdot \Delta\gamma \end{pmatrix} \tag{40}$$

The coordinates of the second ball are symmetrical to the x-axis:

$$\begin{pmatrix} x_C \\ y_C \\ z_C \end{pmatrix} = \begin{pmatrix} x_D \\ -y_D \\ -z_D \end{pmatrix} = \begin{pmatrix} \dfrac{D_{pw}}{2} \cdot \cos\Delta\gamma \\ \dfrac{D_{pw}}{2} \cdot \sin\Delta\gamma \\ \dfrac{P_h}{2\pi} \cdot \Delta\gamma \end{pmatrix} \tag{41}$$

The three-dimensional distance of two adjacent centres is D_{pw}:

$$\sqrt{(x_C - x_D)^2 + (y_C - y_D)^2 + (z_C - z_D)^2} = D_{pw} \tag{42}$$

Thus, $\Delta\gamma$ may be determined if (40) and (41) are applied on (42):

$$\sqrt{(D_{pw} \sin\Delta\gamma)^2 + \left(\dfrac{P_h}{\pi} \cdot \Delta\gamma\right)^2} = D_{pw} \tag{43}$$

According Fig. 6 the number of balls z is:

$$z = \frac{2\pi}{2 \cdot \Delta\gamma} = \frac{\pi}{\Delta\gamma} \tag{44}$$

Approximately, the segment of the ellipse between two centres is straight (see Fig. 6). Its length l_{CD} is:

$$l_{CD} \approx D_w \cdot \cos\psi_{pw} \tag{45}$$

The result for $\Delta\gamma$ is:

$$\Delta\gamma = \arcsin\left(\frac{D_w \cdot \cos\psi_{pw}}{D_{pw}}\right) = \arcsin\left(\frac{D_w \cdot \pi}{\sqrt{\left(D_{pw} \cdot \pi\right)^2 + P_h^2}}\right) \tag{46}$$

The time t_{circ} the ball takes to run one turn around the shaft is:

$$t_{circ} = \frac{l_{pw}}{|\vec{v}_O|} = \frac{\sqrt{\left(D_{pw} \cdot \pi\right)^2 + P_h^2}}{|\vec{v}_O|} \tag{47}$$

When a damage of at least one component occurs it is overrun periodically. This implies forces which excite vibrations that may be assigned to dedicated components. Also the characteristic frequencies of different units of the whole drive feed such as bearings, linear guides and ball screws differ from each other. By the measurement of the ball screw drive the velocity of the balls by which they overrun damages on the nut, the shaft or they pass through the return units may be determined. A location on the runway in the nut will be overrun z times.

$$f_{Nut} = \frac{z}{t_{circ}} = \frac{\pi \cdot |\vec{v}_O|}{\Delta\gamma \cdot \sqrt{\left(D_{pw} \cdot \pi\right)^2 + P_h^2}} \tag{48}$$

A location on the shaft is overrun accordingly:

$$f_{inside} = \left(f_{sp} - f_{circ}\right) \cdot z = \left(f_{sp} - \frac{1}{t_{circ}}\right) \cdot \frac{\pi}{\Delta\gamma} \tag{49}$$

For condition monitoring, f_{Nut} is the frequency by which the balls excite the system when they overrun a damage on the nut. f_{inside} is the frequency by which damages on the shaft are overrun. To meet the requirements of a feed drive it is also interesting to know how much distance is fed during the periodic time. The distance Δx_{Nut} for the nut is:

$$\Delta x_{Nut} = \frac{f_{sp} \cdot P_h}{f_{Nut}} \tag{50}$$

For the shaft the distance Δx_{Sp} is:

$$\Delta x_{Sp} = \frac{f_{sp} \cdot P_h}{f_{inside}}$$ (51)

Equation (38) and equation (39) show that the distances are independent from the rotary speed. Δx_{Nut} and Δx_{Sp} depend only on the measurements of the ball screw. This approach may be used to identify the respective damaged part of the feed drive. It's noticeable that opposed to bearings during an examination the rotary speed doesn't need be constant (Δx_{Sp} and Δx_{Nut} don't depend on frequency or time respectively). For closer examination of sampled signals it's also important to know the characteristic numbers of events per distance. For the shaft and for the nut they are:

$$z_{Nut} = \frac{1}{\Delta x_{Nut}} = \frac{f_{Nut}}{f_{sp} \cdot P_h} \qquad z_{Sp} = \frac{1}{\Delta x_{Sp}} = \frac{f_{inside}}{f_{Sp} \cdot P_h}$$ (52), (53)

In comparison to bearings, the main difference is that a damage on the shaft excites vibrations only while the nut covers the concerning area. So the duration of the according signal will be considerably shorter. Thus a frequency-based analysis is not the best method.

It fits much better to a feed drive's intended use to analyze its behaviour according to position rather than to frequency. Since the characteristic figures (5252), (53) depend on the geometry and the frictional coefficients only. They form the basis for a state detection depending on the position only:

$$z_{Nut}, z_{Sp} \neq f(\omega)$$ (54)

The following measurement's setup was specifically designed according these principles. The acquired signals are no vibrations. Therefore all disturbing effects like interferences do not occur. If anything altering of the feed speed only affects the amplitudes of the measured signals. It never affects the position of the characteristic peaks.

3. METROLOGICAL CAPTURE OF WEAR OF FEED DRIVES WITH BALL SCREWS

3.1. MEASUREMENT SETUP

Exemplarily a ball screw which is typical for machine tools was examined. In fact the contact angle depends on the load. The contact angle and the friction coefficient influence the numbers of events per distance. Fig. 7 shows the characteristic number of events z_{Nut} and z_{Sp} in dependency of the friction coefficients μ_{Nut}, μ_{Sp} and the contact angle α.
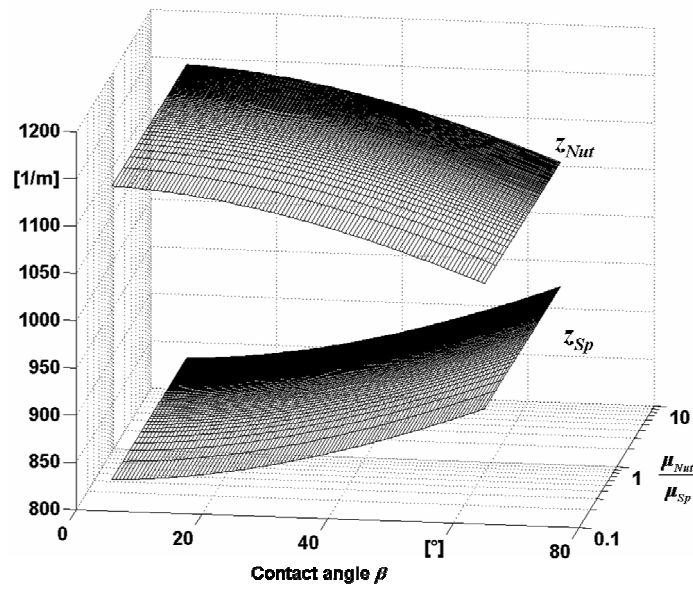
Fig. 7. Spatial resolution of events at the nut z_{Nut} and at the shaft z_{Sp}

The measurements are:

	Contact angle α	
Shaft diameter D_{pw}	32 mm	
Pitch (Lead) P_h	10 mm	
Ball's diameter D_w	6.35 mm	
Contact angle α	60°	
Friction coefficient μ	$\mu_{Nut} = \mu_{Sp}$	
Calculated characteristic event, nut z_{Nut}	723 m^{-1}	
Calculated characteristic event, shaft z_{Sp}	877 m^{-1}	
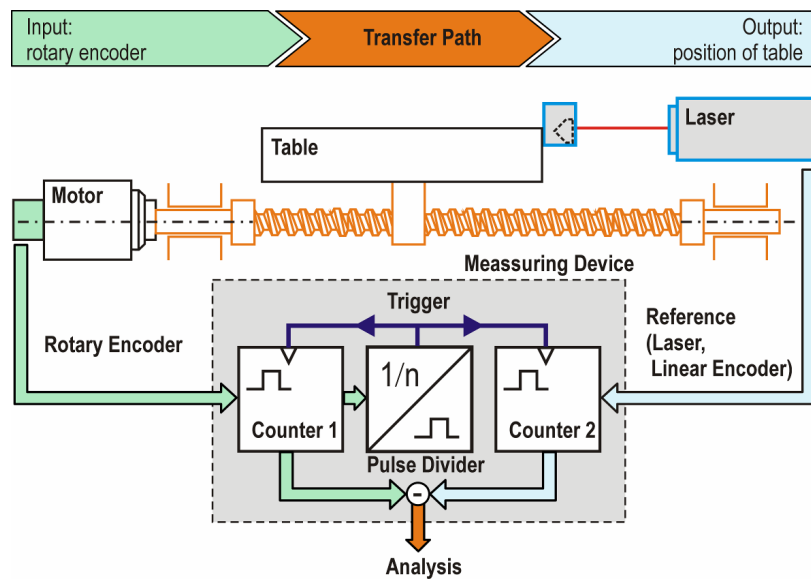
Fig. 8. Measurement setup for spatial decomposition of positioning data

The measurement setup to detect wear of the mechanical components of a feed drive is shown in Fig. 8. The intention is to acquire data at two interfaces of the system. The mechanical components form the transmission path in between.

The input interface of the measurement setup is the rotary encoder of the servo motor. The controller is guided by the rotary encoder. Therefore any inaccuracies of the mechanics may not be compensated by the controller. The other interface is the actual position of the machine table. It may be acquired by a laser interferometer or by a linear encoder. Both units are triggered simultaneously at equally spaced distances. A pulse divider is used to adjust the sampling distance. For a ball screw the highest interesting number of events is z_{Sp}. (According the mathematical derivation Δx_{Sp} will always be lower than Δx_{Nut}.) In order to extract the concerning information from the signals the sampling resolution has to be high enough. Therefore the highest spatial sampling distance may be $\Delta x_{Sp}/2$. For the given ball screw numerically at least 1754 (= 2x877) samples per meter have to be made.

3.2. EXEMPLARY RESULTS

When the positioning error i.e. the difference between the appointed position and the actual position is spatially decomposed, peaks at the characteristic numbers of events are visible. Fig. 9 shows the decomposed signal of a brand new ball screw. The measured peaks coincide exactly with the calculated figures z_{Nut} and z_{Sp}. The distance of the peaks (2) is proportional to the contact angle α, the absolute middle of the two peaks (1) is proportional to the diameters' ratio D_{pw}/D_w. Also clearly visible is the considerably high signal-to-noise ratio (SNR). (To numerically calculate the SNR may be left out here please.)
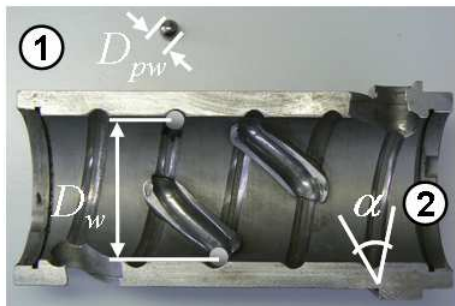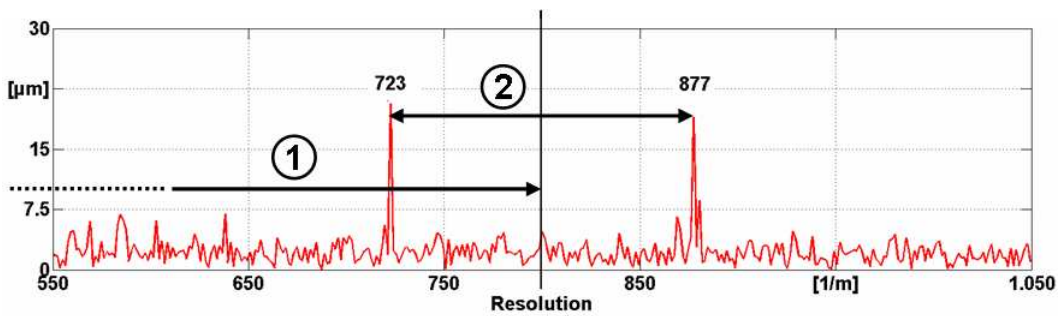
$$\text{①} \quad 1/2 \ \left| z_{Nut} - z_{Sp} \right| \quad \alpha \tag{55}$$

$$\text{②} \quad 1/2 \cdot \left| z_{Nut} + z_{Sp} \right| \quad \frac{D_{pw}}{D_w} \tag{56}$$

Fig. 9. Dependencies of the characteristic peaks of a feed drive with a new ball screw (lifetime < 1 hr)

Fig. 10 shows the charts for two directions. In contrary to frequency based measurements this clearly shows differences for the respective directions. Especially at z_{Nut} the amplitudes are different. This can be assigned to the re-feeding units that are not ambidextrous (see Fig. 10, left). On the other hand the characteristic peaks for the shaft do not differ from each other (see Fig. 10, right). Occasionally, a peak in the middle occurs, that could not be assigned to anything yet (any suggestions anybody?).
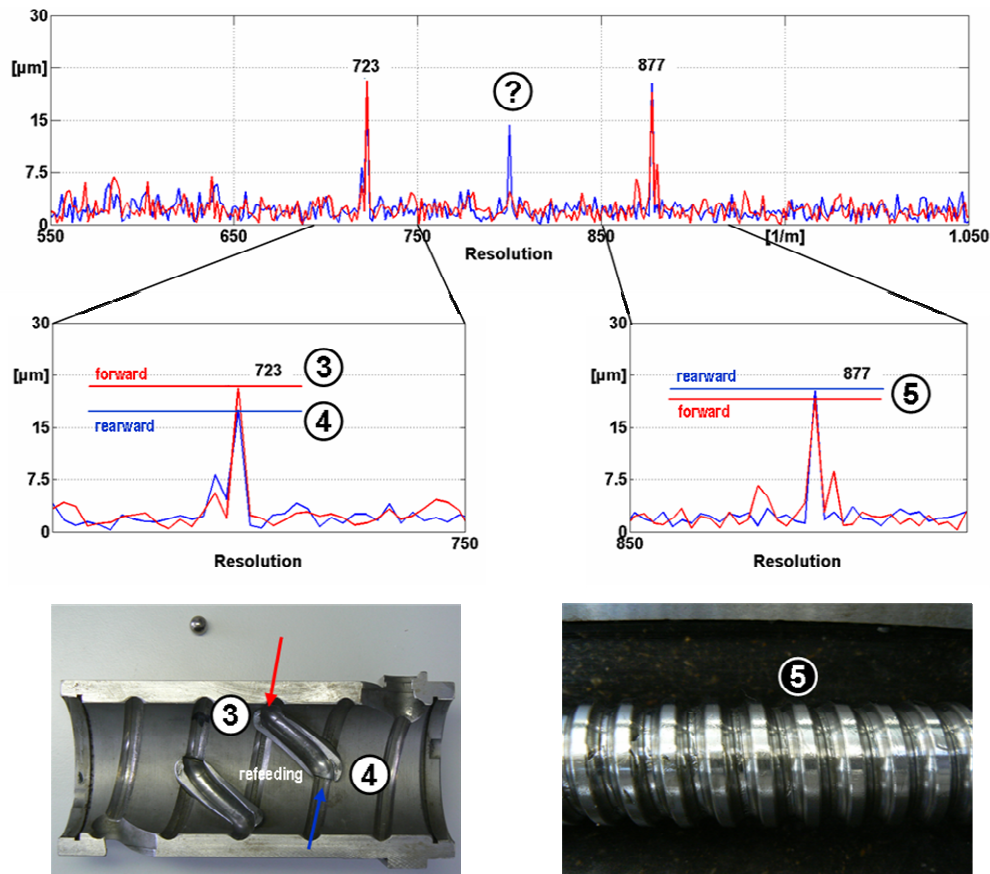
Fig. 10. Significant signals for reverse movement. Influences of the re-feeding (3, 4) and the shaft (5)

Fig. 10 shows that for an unprepared shaft only the peaks of the re-feeding units are different for both directions. In order to test the influences of rough environmental conditions, another shaft was prepared with a weld spot that was reground. Fig. 11 shows the charts before and after damage. On top the positioning errors over the table's position is shown. Below is the decomposition. Now the full range of resolution is shown. Dominant peaks are at 100, 200 and 300 m^{-1}. They can be assigned to the ball screw's lead which is 10 mm ($z_{lead} = 100$ m^{-1} respectively). Since the servo controller is considerably powerful, the position of the table (i.e. the rotary angle of the motor, to be more precisely) is controlled well (The author's first measurements evidence that the motor's torque rises accordingly at a much higher rate). The signal to noise ratio seems to be considerably bad. The according positioning error is considerably small (top). But the decomposition shows that SNR is still

very good. The concerning peaks of the damaged shaft (blue, bottom) still coincide perfectly with the new ones (red, bottom).
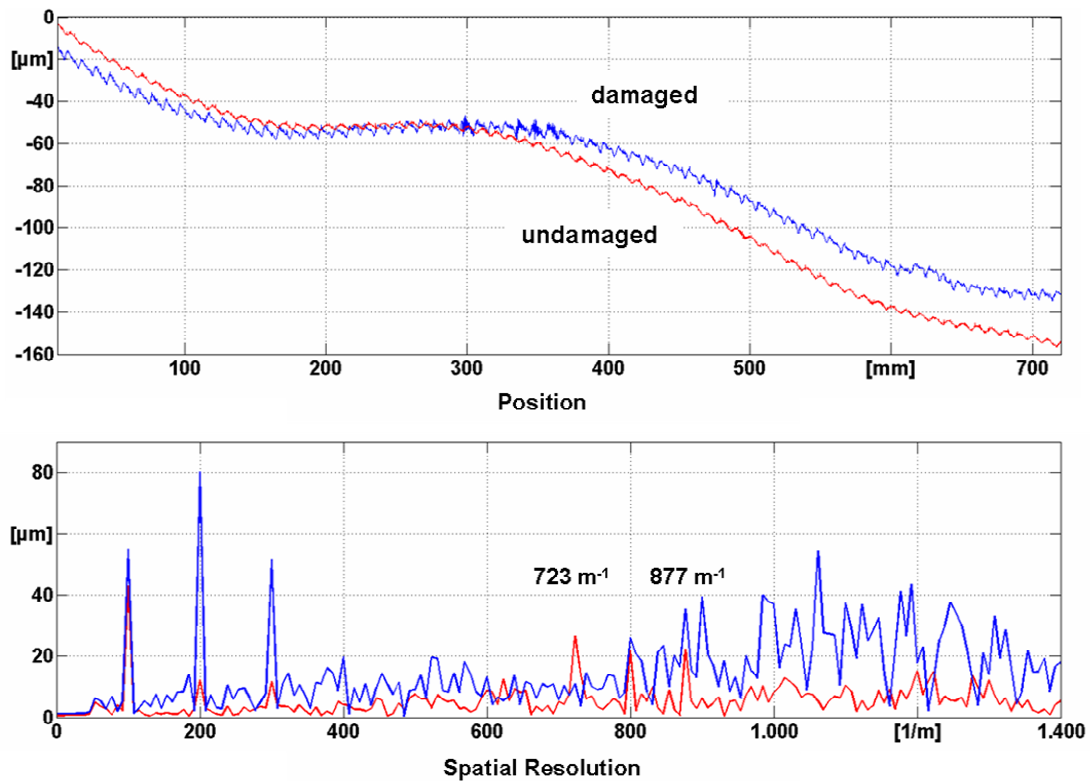

Fig. 11. Positioning error of a feed drive with a ball screw (top). The spatial decomposition (bottom) shows characteristic patterns

In Fig. 11 peaks at the calculated figures z_{Sp} (877 m^{-1}) and z_{Nut} (723 m^{-1}) are visible. As expected, the peak of the damaged shaft rises considerably. Therefore the positioning error between 300 and 400 mm can be assigned to the shaft. The length of the signal (blue, top) matches exactly the nut's length (100 mm). That's the position range while the nut covers the damage. It's remarkable, that the damaged shaft shows high peaks at 200 m^{-1} and 300 m^{-1} whereas the undamaged shaft has a dominant peak at 100 m^{-1} only.

Fig. 12. Prepared damage on the shaft

The damaged signal's form above ~900 m^{-1} is caused by the damage's geometry (see Fig. 12). It's obvious, that the peaks at low resolution are easy to assign to the lead (pitch).

3.3. PERFORMANCE OF THE METHOD

To get an impression of the method's performance, the ball screw drive's measurement was compared to the signals. First calculations showed that the nominal figures of the ball screw drive do not match the signals (*how* they match: see Fig. 9). Especially, the given figure of the nominal diameter was not correct. In order to measure it, cylinders with different diameters sized to match the inside of the ball screw nut were produced. Thus the actual diameter is determined. It's also not common (yet?) for ball screws to give the contact angle in a manufacturer's catalogue (for bearings it is long since). Also it was assumed, that the ball's diameter is 6.35 mm. That also had to be corrected. Actual figures of the measured ball screw are:

Shaft diameter D_{pw}	32.3 mm
Pitch (Lead) P_h	10 mm
Ball's diameter D_w	6.34 mm
Contact angle α	~60° (still difficult to measure)
Friction coefficient μ	$\mu_{Nut}=\mu_{Sp}$
Calculated characteristic event, nut	z_{Nut} 723 m^{-1}
Calculated characteristic event, shaft	z_{Sp} 877 m^{-1}

To prove the statements numerically, the given figures were slightly altered and fed into the model. The resulting characteristic peaks are shown in Fig. 13.
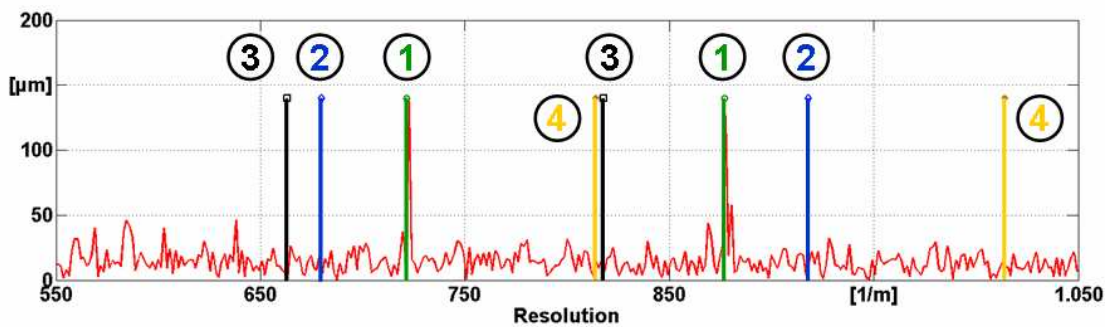

Fig. 13. Varying results for different ball screw's measurements are compared with the signal

The following ball screw measurements were fed into the model:
1. D_{pw}=32.3 D_w=6.34 α=60° z_{Sp}=877m^{-1} z_{Nut}=723m^{-1} (act. values)
2. D_{pw}=30.0 D_w=6.34 α=60° z_{Sp}=918m^{-1} z_{Nut}=680m^{-1} (nom. values)
3. D_{pw}=32.3 D_w=6.34 α=40° z_{Sp}=819m^{-1} z_{Nut}=664m^{-1} (assumed)
4. D_{pw}=37.0 D_w=6.35 α=60° z_{Sp}=1014m^{-1} z_{Nut}=814m^{-1} (assumed)

Fig. 13 shows that the model responds very accurately to any alteration of the geometrical measurements i.e. its peaks are clearly separated (refer to Fig. 9). Mathematically the susceptibilities of the model may be calculated:

$$susc. = \frac{\partial z_{Sp}, \partial z_{Nut}}{\partial \alpha, \partial (D_{pw} / D_w)} \tag{57}$$

Alas MatLab got stuck in this very moment. So no diagram may be shown here. It's of course also difficult, to conduct the according experiments, since the geometry may not be altered deliberately. Different ball screws only give a few samples (that's waste of time).

The ruggedness of the method is evaluated by different feed speed profiles used to sample the data. Then the correlation of the according different signals is calculated. That shows the limits of altering speed's ranges. The results may be mapped on a machined product's geometry. Fig. 14 illustrates the approach. Symbolically a feed speed profile is shown (top) during that a vibration based data acquisition is possible while producing. It's obvious that a wear detection is difficult, when both axis (of the same design and measurements, to make the setup even worse) move at the same time. The signals are very difficult to separate if vibration sensors are used. A diagnosis of real machines should not be based on fixed additional sensors at all (consider noise path analysis!). Move the sensors.
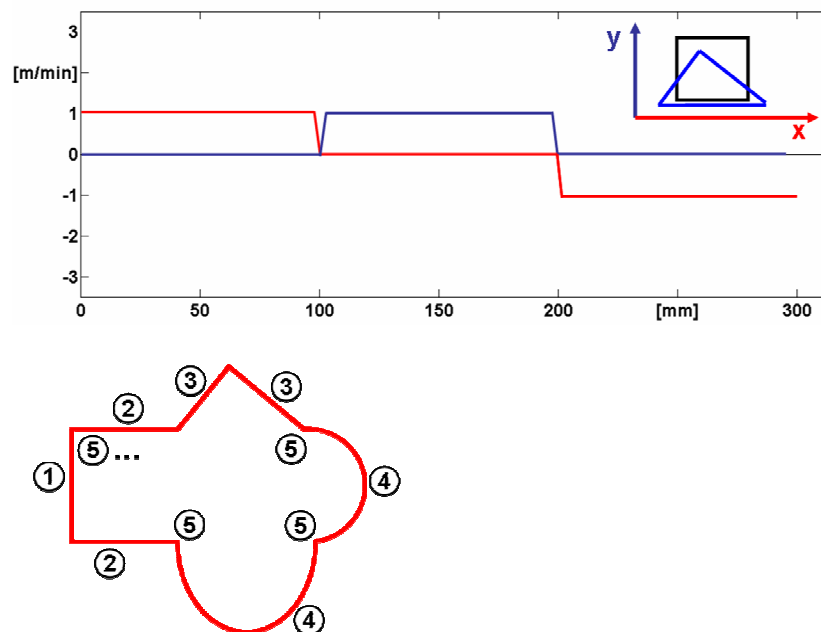

Fig. 14. Feed speed profile for vibration based analysis (top) and contour for position-based analysis (bottom)

On the other hand, an arbitrary contour may be exploited (bottom). If the TCP moves at 1, 2 and 3 the speed is constant. At 4 it is sinusoid and ellipsoid. That's already problematic for vibration based approaches. At 5 phenomena like hysteresis (loosening,

stiffness…) may be detected *and* quantified (see Fig. 10, reversing feed). That's nearly impossible by vibration. Also many errors may only be detected if the machine is excited accordingly. For vibration the excitation (feed speed, motor noise, chirp) is always bound to the mathematics. Nonlinearities (Fig. 14, 5) render these fourier-transformed signals useless.

4. CONCLUSIONS AND PROSPECTS

So, what to conclude? What's left to be said? Too much and too few! The numerical performance is far superior to any vibration based approach. The SNR is also superior. Vibration based methods are not appropriate to detect similar symptoms when the feed speed is reversed. In neither direction even the ball screws lead (pitch) is depicted! Nonlinearities bear important information that is not exploited by vibration. This position based approach uses both, linearities *and* nonlinearities.

The advantages of the presented approach are that only one physical unit is needed, no error prone complex model is used and the feed speed may alter. For the operator of the machine the positioning accurateness is a criterion that he can use directly. Everybody in the business is familiar with it. It's easy for him to set limits that are appropriate to his requirements. The characteristic figures must not be calibrated but they depict the current state (of wear) directly. Self-imposed prerequisites were to use the machine's inherent functionalities only (On board diagnosis). These prerequisites are met. Since it's widely not necessary to use a constant feed speed for the data acquisition, data may be sampled during the normal operation of the machine. At least if the machine moves in idle. As mentioned above, the characteristic numbers of events are independent from the feed speed. Currently, experiments are conducted by the author to find out how much an altering feed speed influences the amplitudes of the characteristic figures when the machine is moved in idle. Next step will be to examine the influence of the running process' forces. Thus a sensor-less (On board) automated condition monitoring based on the presented approach may be totally online. *A way for On-board-Online-diagnosis may be opened.* It's also questionable whether the stiffness of the ball screw is principally appropriate to evaluate its state of wear (or its lifetime). The main purpose is to position. So why evaluate it by stiffness rather than by positional accurateness? The positional accurateness is much more susceptible and alters from the very beginning of the lifetime if it's measured accordingly [3]. Only when it's too late for a repair the stiffness alters. A comparison of two methods may be read in [4].

Next steps will be capturing and decomposing of further signals (torque, current) by the presented method. Thus only one positioning sensor is sufficient.

ACKNOWLEDGEMENTS

REFERENCES

[1]   PALMGREN A., 1964**,** *Grundlagen der Wälzlagertechnik.* Stuttgart: Franckhsche Verlagsbuchhandlung.

[2]   WALTHER, M.; BIRENBAUM, C.; MAIER, D., 2010, *Sensorlose automatisierte Verschleißdiagnose an Vorschubsystemen mit Kugelgewindetrieben in Werkzeugmaschinen.* VDI-Tagung Schwingungsanalyse & Identifikation Leonberg, March, 23. & 24. 2010. (*accepted, not published / printed yet*).

[3]   MAIER D., ZIEGLER F., 2009, *Dynamische Fehlermessung erfasst Verschleiß an Vorschubantrieben.* In: MM Maschinen Markt – Das Industriemagazin, Ausgabe, 40/40 - 42.

[4]   VERL A., HEISEL U., MAIER D., WALTHER M., 2009, *Sensorless Automated Condition Monitoring for the Control of the Predictive Maintenance of Machine Tools.* In: Annals of the CIRP, 58/1/375 – 378.